



## Massively Parallel Individually Selecting Configuration Interaction: A Progress Report

P. Stampfuß, W. Wenzel

published in

*NIC Symposium 2001, Proceedings*,  
Horst Rollnik, Dietrich Wolf (Editor),  
John von Neumann Institute for Computing, Jülich,  
NIC Series, Vol. 9, ISBN 3-00-009055-X, pp. 113-122, 2002.

© 2002 by John von Neumann Institute for Computing

Permission to make digital or hard copies of portions of this work for personal or classroom use is granted provided that the copies are not made or distributed for profit or commercial advantage and that copies bear this notice and the full citation on the first page. To copy otherwise requires prior specific permission by the publisher mentioned above.

<http://www.fz-juelich.de/nic-series/volume9>



# Massively Parallel Individually Selecting Configuration Interaction: A Progress Report

P. Stampfuß and W. Wenzel

Institut für Nanotechnologie, Forschungszentrum Karlsruhe  
Postfach 3640, 76021 Karlsruhe, Germany  
*E-mail: wolfgang.wenzel@int.fzk.de*

We report on the progress of our scalable implementation of the configuration-selecting multi-reference configuration interaction method for massively parallel architectures with distributed memory. With this code, calculations with Hilbert spaces containing more than  $10^{12}$  configurations are now routinely feasible on up to 128 processors of the IBM-SP2 and up to 256 processors on the CRAY-T3E. We briefly explain the key ingredients of the parallel implementation and report the results of two illustrative applications, regarding the fast quantum dynamics near the conical intersection of NO<sub>2</sub> and the investigation of reaction pathways of members of the endiyne family, respectively.

## 1 Introduction

In the development of quantum chemical methods for complex molecules, a consensus has emerged that two important effects must be taken into account in a balanced and accurate fashion in order to arrive at quantitatively correct results. First, dynamical correlations, i.e. the mutual influence two electrons exercise on each other when they pass at close distance, must be accounted for. Secondly, one must be able to accommodate the multi-reference nature of the electronic states in many complex molecules. This effect is particularly important in many transition metal compounds where the close proximity of d-energy levels generates a large number of important multiplets. It is also relevant when one wants to describe an entire potential energy surface, where bond-breaking or bond-rearrangements can occur. An adequate treatment of multi-reference effects is mandatory for the quantitative treatment of electronically excited states. Meeting the needs of both these requirements simultaneously is responsible for the high cost of accurate quantum chemical calculations.

For many years the multi-reference configuration interaction method (MRCI) has been one of the benchmark tools for highly accurate calculations of the electronic structure of atoms and molecules<sup>1-3</sup>. Due to its high computational cost, however, applications of the MRCI method remain constrained to relatively small systems. For this reason the configuration-selective version of the MRCI-method (MRD-CI), introduced by Buenker and Peyerimhoff<sup>4-6</sup>, has arguably become one of its most widely used versions. Even within this approximation, the cost of MRCI calculations remains rather high<sup>7-12</sup>. In order to further extend the applicability of the method, it is thus desirable to employ the most powerful computational architectures available for such calculations. Here we report on the progress of the first massively parallel, residue-driven implementation of the MRD-CI method for distributed memory architectures.

In this manuscript we focus on the details of the implementation of the method and provide timings for benchmark applications that demonstrate the scalability of the method for up to 128 nodes for Hilbert spaces of dimension up to  $5 \times 10^9$  of which up to  $5 \times 10^6$

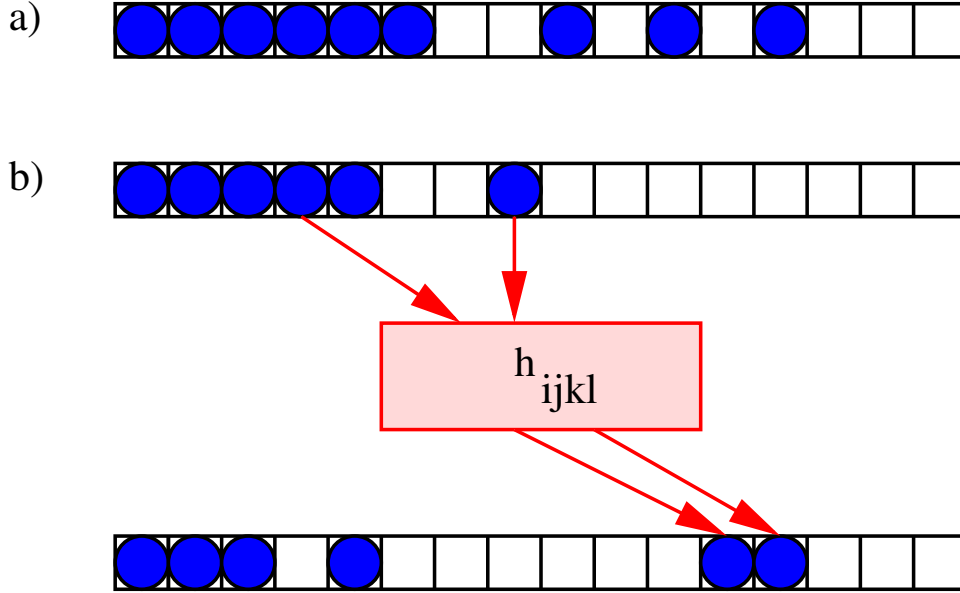


Figure 1. Schematic representation of (a) a 9-electron configuration and (b) a pair hopping process mediated by a term of eq. 1 between two such configurations.

elements were selected for the variational wavefunction<sup>13</sup>. The determinant based code we report here was developed in an object oriented implementation using C++ as the implementation language.

## 2 Method and Implementation

### 2.1 Configuration Interaction Methods

The electronic structure of a many-electron system is described by a many-electron wavefunction that can be represented as a weighted average of many-electron configurations. The set of permissible configurations is called the *Hilbert space* of the system. In each configuration (see Figure (1) (a)), each electron occupies one of many possible orbitals (that are chosen from a finite basis). According to the rules of quantum mechanics each orbital can be occupied by at most one electron. In the presence of electrostatic interactions in molecules, the electrons may hop from one orbital pair to another, according to a *Hamilton operator*

$$H = \sum_{ij} h_{ij} c_i^\dagger c_j + \sum_{ijkl} h_{ijkl} c_i^\dagger c_j^\dagger c_k c_l, \quad (1)$$

where the symbol  $c_i$  represents the operation to remove an electron in orbital  $i$  from a given configuration and  $c_i^\dagger$  creates an electron in this orbital if none previously existed.  $h_{ijkl}$  represents the hopping amplitude for this process (see Figure (1)(b)). The energy of a many

electron wavefunction is computed by applying the above operator to the wavefunction, thus creating another weighted average of configurations (with changed coefficients) and to sum the pointwise products of the coefficients of identical configurations in the original and the transformed wavefunction. The individual configurations are thus interacting via the Hamilton operator, methods that explicitly compute these interactions belong to the family of *configuration interaction* (CI) methods.

In all CI methods the coefficients of the weighted average that represents the wavefunction are iteratively adjusted to minimize the energy of the resulting state. The variational theorem of quantum mechanics assures us that the many-body wavefunction with the lowest energy is that of the desired ground state of the system. To obtain accurate results, one would like to choose a basis that is as large as possible to describe the many-body wavefunctions. However, if all electrons are permitted to occupy all orbitals — a method known as full CI — the number of configurations grows as  $N!/[n_e!(N - n_e)!]$  with the number of orbitals  $N$  and the number of electrons  $n_e$ . For benzene, as a small example ( $n_e = 42$ ), in a basis of just 100 orbitals, this would result in an astronomical number of  $10^{28}$  configurations. Fortunately, the many body wavefunction is often dominated by only a few configurations, the so called reference configurations. Applying the Hamilton operator to those, generates a new set of *excited configurations* that are the most important in the description of the system. In the *multi-reference configuration interaction method* (MRCI) only the reference and the excited configurations are included in the Hilbert space. Their number grows as  $N_{\text{ref}} \times n_e^2 \times N^2$  and the number of possible transitions generated by equation (1) grows as  $N_{\text{ref}} \times n_e^2 \times N^4$ , i.e. with the sixth power of the number of electrons (we assume that the number of orbitals is also proportional to the number of electrons). Returning the example of benzene, the calculation can still include  $10^9$  configurations, with  $O(10^{11})$  matrix elements.

Instead of explicitly considering all possible configurations in the MRCI Hilbert space one can reduce the computational effort further by dynamically selecting only those configurations that are important in the actual calculation. In this method, called MRD-CI<sup>5</sup>, only the most important configurations of the interacting space of a given set of primary configurations are chosen for the variational wavefunction, while the energy contributions of the remaining configurations are estimated on the basis of second-order Rayleigh-Schrödinger perturbation theory<sup>14,9,5</sup>. Since the variationally treated subspace of the problem consists of only a fraction of the overall Hilbert space, the determination of eigenstates in the truncated space requires far less computational effort.

Even in this approximation the computational requirements remain large even for relatively small molecules. It is therefore sensible to exploit the most powerful computational resources available to perform these calculations, i.e. massively parallel computers with distributed memory. Unfortunately efforts of chemists and physicists to use these machines for methods of wavefunction-based theoretical chemistry, have so far been met by-and-large with difficulties. The reasons for these difficulties are often the lack of intuitive algorithms which coordinate the calculation on a large number of processors while keeping the communication efforts under control. For MRCI based applications, both the data for the wavefunction and the Hamiltonian coupling constants  $h_{ijkl}$  are so large that they cannot be stored on a single node. Hence both pieces of data must be moved around during the calculation, which must be coordinated on *all nodes* of the machine in such a way that no idle periods occur on *any node* of the machine. To generically address the problem for

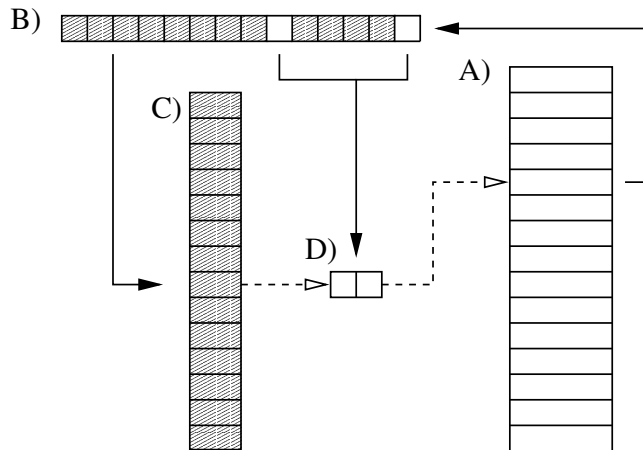


Figure 2. Schematic representation of the two-particle residue-tree. For each element of the configuration-list (A) all possible two-particle residues are constructed. In the configuration illustrated in (B) each box represents one occupied orbital, the shaded region corresponds to the residue and the two white boxes to the orbital pair. The  $(n_e - 2)$ -electron residue configuration is looked up in the residue-tree (C), where an element (D) is added that encodes the orbitals that were removed, information regarding the permutation required and the index of the original configuration in the configuration list. Solid arrows in the figure indicate logical relations ships, dotted arrows indicate pointers incorporated in the data structure. The residue-list, along with all elements must be rebuilt once after each expansion loop, the effort to do so is proportional to product of  $n_e^2$  with the number of configurations. The number of matrix elements encoded in a single element of the residue-tree is proportional to the *square of the number of entries* of type (D).

the unstructured wavefunction in MRD-CI, we have developed a *transition residue* driven matrix element evaluation scheme that accomplishes this task in an *explicitly scalable fashion, independent of the number of nodes, the number of electrons and the number of orbitals*. In the following we will briefly outline the key ideas of this approach, report the scaling behavior in benchmark calculation and summarize two illustrative application of the program.

## 2.2 Parallel Implementation

In order to compute the matrix elements of the Hamilton operator between two configurations we exploit an enumeration scheme in which each matrix element between two configurations is associated with the subset of orbitals that occur in both the target and the source configuration. This unique subset of orbitals is called the *transition residue* mediating the matrix element and serves as a sorting criterion to facilitate the matrix element evaluation on distributed memory architectures. For a given many-body state, we consider a tree of all possible transition residues as illustrated in Figure (2). For each such residue we build a list of *residue-entries*, composed of the orbital-pairs (or orbital for a single-particle residue) which combine with the residue to yield a selected configuration and a pointer to that configuration. While the number of transition residues is comparatively small, the overall number of residue-entries grows rapidly (as  $N_{selected} n_e^2$ ) with the number of configurations  $N_{selected}$  and the number of electrons  $n_e$ . Once the residue

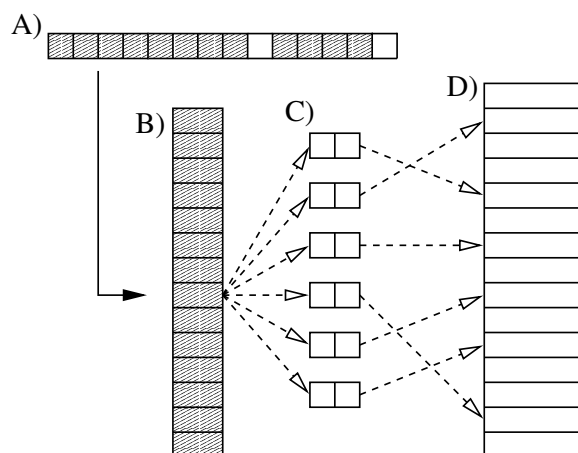


Figure 3. Schematic representation of the computation of two-particle matrix-elements in the expansion step using the residue-tree. For a given configuration (A) we form all two-particle residues, which are looked up in the residue tree. In the configuration illustrated in (A) each box represents one occupied orbital, the shaded region corresponds to the transition residue and the two white boxes to the orbital pair. The  $(n_e - 2)$ -electron residue configuration is looked up in the residue-tree (B). Each orbital pair (C) associated with the residue encodes a matrix element with an element of the configuration list (D). The orbital indices of the required integral are encoded in the orbital pairs in (C), the coefficient of the source configuration is looked up directly in (D). Only one lookup operation is required to compute all matrix elements associated with the given transition residue and only the subset of matrix elements that lead to selected source-configurations are constructed.

tree is available the evaluation of the matrix elements is very efficient, because all matrix elements associated with a given transition residue can be evaluated on a single node.

In order to demonstrate the scalability of the implementation we have conducted benchmark calculations for typical applications of the program, concerning the evaluation of the importance of the triple and quadruple excitations for the potential energy surfaces of the oxygen molecule ( $10^9$  configurations,  $1.8 \times 10^6$  selected) and the excited states for benzene ( $1.3 \times 10^9$  configurations,  $1.6 \times 10^6$  selected), respectively (for details see<sup>13</sup>).

Figure (4) shows the total computational effort (excluding the time to read the integral file) of the aforementioned scaling runs as a function of the number of nodes. In these plots, the computational effort for all logic-steps are subsumed in one category, the expansion loop and the iteration loop constitute the other main components of the program. For benzene we find almost perfect scaling from 48 to 128 nodes, the overall speedup factor from 64 to 128 nodes is 1.86. For the benchmark calculation of  $O_2$  a more pronounced increase in the overall computational effort is observed in going from 32 to 128 nodes, in particular in with the last doubling from 64 to 128 processors.

### 3 Applications

The algorithm described above has been used for a number of applications, e.g. the photochemistry of  $NO_2$ , the computation of electron affinities of oxides, the spectroscopy of transition-metal dihalides, the elucidation of the electronic structure of benzofuroxane and

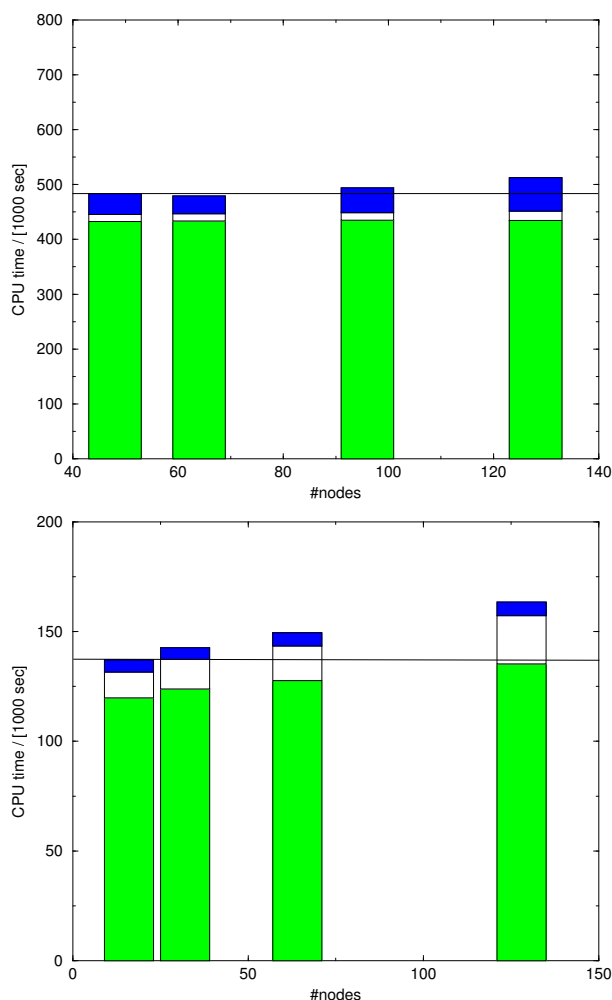


Figure 4. Total CPU time in (sec) for the fully converged calculation of the ground state of the two benchmark calculations described in the text as a function of the number of nodes. A straight line indicates perfect scaling of the computational effort with the number of nodes. The shaded areas in the bars, from top to bottom, indicate the contributions of the matrix element evaluation, logic and the selection loop, respectively.

recently the investigation of single transition metal centers in biomolecules, e.g. azurin. Here we illustrate its usefulness with two examples, regarding the conical intersection of  $\text{NO}_2$  and the reaction mechanisms of a family of potential anti-cancer drugs.

### 3.1 Conical Intersection in $\text{NO}_2$

Vibronic interactions between different electronic potential energy surfaces are a generic feature of polyatomic molecules. Such interactions are strong for near-degenerate or degenerate electronic states, and the spectroscopy and dynamics of a molecule are strongly



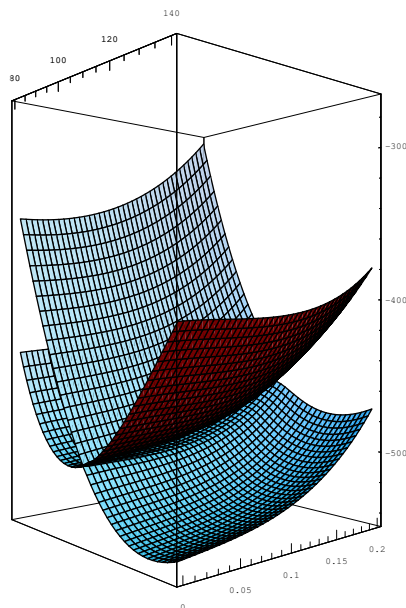


Figure 5. Two dimensional cut through the three-dimensional adiabatic potential energy surface of the  $\tilde{X}^2A_1$  and  $\tilde{B}^2B_1$  electronic states of  $\text{NO}_2$  in the vicinity of the conical intersection computed using the quasi-diabatic representation of the underlying potential energy surfaces discussed in the text. The mean distance was  $r = 1.25$  Å. The two horizontal axes measure the angle and the asymmetric stretch respectively. The vertical axis shows the energy in millihartree with respect to an offset of  $E_0 = -204.0$  a.u.

influenced by the associated non-adiabatic couplings<sup>15–18</sup>. A typical scenario in polyatomic systems is the occurrence of *conical intersections* of potential energy surfaces, where two electronic states become degenerate along a hypersurface of the PES. In dealing with such a system theoretically one needs to go beyond the Born-Oppenheimer approximation and solve complex coupled differential equations in order to monitor the nuclear motion simultaneously on more than one electronic state. Although this concept is well known in the literature, the actual construction of diabatic electronic states for a polyatomic system is still a highly difficult task and has only partly been achieved to date<sup>19</sup>).

$\text{NO}_2$  is a well known triatomic molecule which has an outstandingly complex spectroscopy. Most of the investigations on this system to date are concerned with understanding the highly dense spectral lines in its optical spectra<sup>20–25</sup>. Adiabatic three-dimensional potential energy surfaces were computed using the configuration-selecting multi-reference configuration-interaction method<sup>5</sup> with the cc-pVTZ basis set<sup>26</sup>. The calculations were carried out in  $C_s$  symmetry using state-averaged approximate natural orbitals generated with MR-BWPT<sup>27,28</sup>. A two-dimensional section through the computed adiabatic PES in this representation is shown in Figure (5), its features were found to be in excellent agreement with the available experimental data.

Employing these coupled  $\tilde{X}^2A_1/\tilde{A}^2B_2$  diabatic potential energy surfaces Mahapatra and Köppel calculated the photodetachment spectrum of  $\text{NO}_2^-$  for a transition to the  $\tilde{A}^2B_2$  electronic state of  $\text{NO}_2$  with the aid of a time-dependent wave packet propagation scheme.

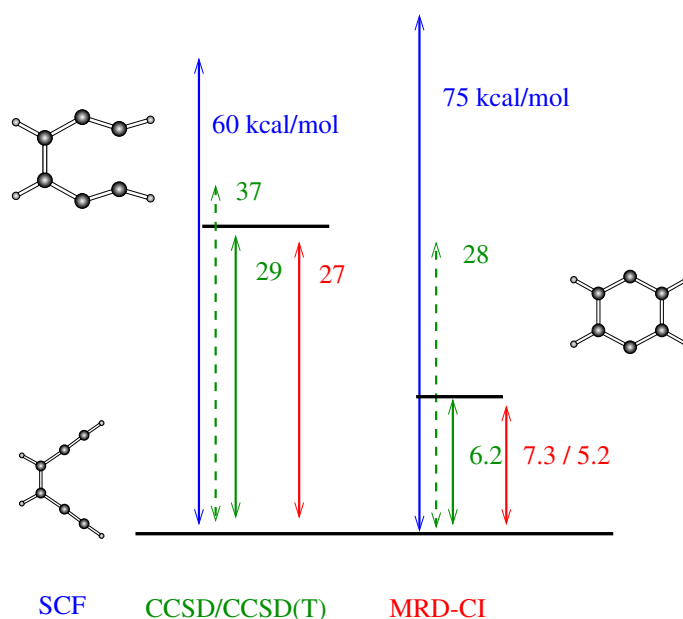


Figure 6. Schematic representation of the energetics (electronic contribution only) of the cyclization reaction of enediyne to para-dihydrobenzene in a cc-pVDZ basis set computed by a variety of methods. For details see the discussion in the main text, all energies are in kcal/mol relative to the educt.

The details of their investigation are beyond the scope of this report (see<sup>29</sup>) so that only the most important points are summarized here. The  $\tilde{A}^2B_2$  photoelectron spectrum originates right at the onset of the nonadiabatic regime (the  $\tilde{X}^2A_1/\tilde{A}^2B_2$  cusp occurs  $\sim 0.08$  eV above to the minimum of the  $\tilde{A}^2B_2$  electronic state) and it is highly sensitive to the strength of the nonadiabatic interaction. The photoelectron spectrum obtained for the uncoupled  $\tilde{A}^2B_2$  electronic state reveals progression along the bending vibrational mode of  $\text{NO}_2$ ; the peaks are  $\sim 0.1$  eV apart, which is about a quantum of bending vibration of  $\text{NO}_2$  in the  $\tilde{A}^2B_2$  state. The  $\tilde{A}^2B_2$  photoelectron spectrum obtained including the coupling to the  $\tilde{X}^2A_1$  state reveals main progression of lines along the bending vibrational mode of  $\text{NO}_2$  and in addition clustering around each main line is an effect of nonadiabatic interactions on this photoelectron band. Due to these interactions the high energy vibrational states of  $A_1$  symmetry mix with the low-lying vibrational states of  $B_2$  symmetry and the resulting spectral lines are clumped into groups of non-overlapping resonances. To compare this coupled state spectrum with the experimental recording of Weaver *et al.*<sup>23</sup> we convoluted it by a Lorentzian function with FWHM of 28 meV. The resulting convoluted spectrum compares well with the experimental one.

### 3.2 Enediyne

The enediyne family of molecules has been investigated for some time because these molecules can undergo a cyclization reaction to a para-dihydrobenzene derivative that is capable of lysing cellular DNA and hence cause cell death<sup>30</sup>. This property of the molecules,

if selectively activated in diseased or cancerous cells offers the possibility to use members of this family as cell-specific drugs against such diseases. The ultimate goal is to design a compound that in cancerous cells will spontaneously undergo cyclization at physiological conditions and thus kill diseased cells. In order to predict the effectiveness of specific compounds it is important to understand the electronic structure of educt and product of the cyclization reaction as well as the height of its barrier. Possible applications of derived compounds aside the quantum chemical description of the cyclization reaction proves difficult and interesting because of the strong change in the electronic structure of the molecule during the reaction.

We have therefore undertaken a set of MRD-CI benchmark calculation into the Bergman cyclization of the simplest member of the enediyne family. We have performed a systematic investigation of these compounds using cc-pVDZ, cc-pVTZ and cc-pVQZ basis sets (the largest ever considered for these molecules). As illustrated in Figure (6) we have been successful in establishing that MRD-CI reproduces the CCSD(T) results. The transition state (using the CCSD geometry) is predicted 2kcal/mol less than by CCSD(T), the product lies 7.2 / 5.8 kcal/mol above the educt depending on whether a multi-reference Davidson correction is applied in the MRD-CI calculation or not. This brackets the values of the CCSD(T) calculation.

## 4 Summary

In recent years we have developed an explicitly scalable implementation of an established quantum chemical method that permits the investigation of complex chemical processes with high accuracy. Presently this program permits the routine treatment of molecules containing about 100 correlated electrons at benchmark accuracy and thus allow the application of this technique to new areas of scientific investigation, such as the analysis of enzymatic reaction that are catalyzed by transition metal centers. The first set of such calculations, aiming to elucidate the enzymatic reaction mechanism of isopenicillin-N-synthase with the help of a new inhibitor-protein complex are presently under way in our group.

*Acknowledgments:* Part of this work was supported by DFG Grants KEI-164/11-2, WE 1863/10-1 and WE 1863/11-3. We acknowledge the use of computational resources at the NIC and the RZ Karlsruhe.

## References

1. B. O. Roos. *Chem. Phys. Letters*, 15:153, 1972.
2. B. O. Roos and P. E. M. Siegbahn. The direct configuration interaction method. In H.F. Schaefer III, editor, *Methods of Electronic Structure Theory*, page 189. Plenum, New York, 1994.
3. I. Shavitt. In H. F. Schaefer III, editor, *Modern Theoretical Chemistry*. Plenum, New York, 1977.
4. R. J. Bunker and S. Peyerimhoff. *TCA*, 12:183, 1968.
5. R. J. Bunker and S. D. Peyerimhoff. *Theor. Chim. Acta*, 35:33, 1974.
6. R. J. Bunker and S. D. Peyerimhoff. *Theor. Chim. Acta*, 39:217, 1975.

7. R. J. Buenker and S. D. Peyerimhoff. *New Horizons in Quantum Chemistry*. Reidel, Dordrecht, 1983.
8. J. L. Whitten and M. Hackmeyer. *J. Chem. Phys.*, 51:5548, 1969.
9. B. Huron, J.P. Malrieu, and P. Rancurel. *J. Chem. Phys.*, 58:5745, 1973.
10. R. J. Harrison. *J. Chem. Phys.*, 94:5021, 1991.
11. S. Krebs and R. J. Buenker. *J. Chem. Phys.*, 103:5613, 1995.
12. M. Hanrath and B. Engels. *CP*, 225:197, 1997.
13. P. Stampfuß, H. Keiter, and W. Wenzel. *J. Comput. Chem.*, 20:1559, 1999.
14. Z. Gershgorin and I. Shavitt. *Int. J. Quantum Chem.*, 2:751, 1968.
15. H. Köppel, W. Domcke, and L. S. Cederbaum. *Adv. Chem. Phys.*, 57:59, 1984.
16. R. L. Whetten, G. S. Ezra, and E. R. Grant. *Annu. Rev. Phys. Chem.*, 36:277, 1985.
17. I. B. Bersuker and V. Z. Polinger. *Vibronic Interactions in Molecules and Crystals*. Springer, Berlin, 1989.
18. W. Domcke and G. Stock. *Adv. Chem. Phys.*, 100:1, 1997.
19. L. S. Cederbaum T. Pacher. *Adv. Chem. Phys.*, 84:293, 1993.
20. G. D. Gillispie, A. Khan, A. C. Whal, R. P. Hosteney, and M. Krauss. *J. Chem. Phys.*, 63:3425, 1975.
21. C. F. Jackels and E. R. Davidson. *J. Chem. Phys.*, 64:2908, 1976.
22. C. F. Jackels and E. R. Davidson. *J. Chem. Phys.*, 64:2941, 1976.
23. A. Weaver, R. B. Metz, S. E. Bradforth, and D. M. Neumark. *J. Chem. Phys.*, 90:2070, 1989.
24. E. Leonardi and C. Petrongolo. *J. Chem. Phys.*, 106:10066, 1997.
25. S. Mahapatra, H. Köppel, and L. S. Cederbaum. *J. Chem. Phys.*, 110:5691, 1999.
26. T. H. Dunning. *J. Chem. Phys.*, 90:1007, 1989.
27. W. Wenzel, M. M. Steiner, J. W. Wilkins, and K. G. Wilson. *Int. J. Quantum Chem.*, S30:1325, 1996.
28. W. Wenzel and M. M. Steiner. *J. Chem. Phys.*, 108:4714, 1998.
29. S. Mahapatra, H. Köppel, L.S. Cederbaum, P. Stampfuß, and W. Wenzel. *Chem. Phys.*, 259:211, 2000.
30. R. Gleiter and D. Kratz. *Angew. Chemie*, 105:884, 1993.